Grafting carbon nanotubes onto carbon fibres doubles their effective strength and the toughness of the composite

Luca Lavagna[1], Daniele Massella[1], Maria F. Pantano[2], Federico Bosia[3], Nicola M. Pugno[2,4,5], Matteo Pavese[1(*)]

[1]*Department of Applied Science and Technology, Politecnico di Torino, Corso Duca degli Abruzzi 24, 10129 Torino, Italy*

[2]*Laboratory of Bio-Inspired and Graphene Nanomechanics, Department of Civil, Environmental and Mechanical Engineering, University of Trento, Via Masiano 77, I-38123 Trento, Italy*

[3]*Department of Physics and Nanostructured Interfaces and Surfaces Interdepartmental Centre, Università di Torino, Via P. Giuria 1, 10125 Torino, Italy*

[4]*School of Engineering and Materials Science, Queen Mary University of London Mile End Road E1-4NS, London, UK*

[5]*KET Lab, Edoardo Amaldi Foundation, Italian Space Agency, Via del Politecnico snc, 00133 Rome, Italy*

(*) Corresponding author

Abstract

Bioinspiration can lead to exceptional mechanical properties in a number of biological materials as a result of their internal structure. In particular, the hierarchical arrangement of nano- to macro-components can bring to complex energy dissipation mechanisms and unprecedented resistance to crack growth. In this work, we propose to exploit this approach, combining in a multiscale composite structure carbon nanotubes with conventional carbon fibre reinforcements in a polyvinyl butyral matrix. We show that grafting the nanotubes onto the carbon microfibres improves their interface properties with the matrix considerably, effectively doubling their apparent strength. At the same time, the addition of nanotubes to microfibre reinforcements helps to improve the composite toughness, reaching more than twice the value for the conventional, non-hierarchically reinforced composite. Numerical simulations and fracture mechanics considerations are also provided to interpret the results.

1. Introduction

Recent developments in nanotechnology have opened the way to a new generation of polymer matrix composites that employs nanomaterial fillers to enhance specific mechanical, electrical and thermal properties. Very often, these nanofillers are based on carbonaceous materials such as graphene or carbon nanotubes (CNTs), although clays are also widely used [1]. The main issue in the employment of carbon nanomaterials in composite manufacturing lies in the difficulty in endowing the final material with the superior properties of the nanofiller , i.e. transferring nanoscale properties to a macroscopic material [2].

Perhaps the best examples of how microscale and nanoscale morphologies can be arranged into a macroscopic material to yield exceptional mechanical properties are provided by natural systems [3]. For example, bone composite structure comprises different hierarchical levels, from macro to nano scale and it has been observed that effective stress transfer along the different length scales leads to exceptional mechanical performance from relatively weak constituents [4,5]. These observations have led to significant interest in the development of so-called "bioinspired materials" i.e. artificial materials that mimic some of the specific structures observed in nature, in order to achieve similar properties [6]. When mimicking the characteristics of natural hierarchical assemblies it is possible to further improve the overall mechanical performance of the obtained structures by employing constituent materials that displays a high intrinsic strength [7]. Carbonaceous materials provide great potential for this type of application because of the high strength due to the presence of carbon-carbon bonds in their structures, and are available in several sizes and morphologies (fibres, nanotubes, graphene, etc.), allowing the creation of a multiscale, hierarchical structure [8,9]. Several studies have been conducted on the manufacturing of multiscale-reinforced materials based on carbon fibres (CFs) and CNTs to reinforce polymeric matrices in composites [10].

A simple method to prepare CF-CNT multiscale composites consists in dispersing the CNTs in the polymer and then producing a fibre reinforced polymer (FRP) by common manufacturing techniques such as resin transfer molding or infusion/impregnation [11,12]. Generally speaking, to disperse nanofillers in the matrix of a FRP allows to combine the simplicity of production with an improvement of the mechanical properties of the composite that are dominated by the matrix [13]. Instead, fibre-related properties are not influenced. Major limits of these techniques are the low amount of nanofiller that can be loaded in the matrix without altering the viscosity (which can compromise the FRP production process) and the limited improvement of fibre-dominated properties such as tensile strength [14].

Another approach that allows to produce multiscale "hierarchical" composite materials is to combine CFs and CNTs in a multiscale reinforcement for the polymeric matrix [15]. The synthesis of the multiscale reinforcement can occur by directly growing the CNTs onto the CFs by chemical vapor deposition or by chemical grafting of the CNTs on the fibre surface [16]. Since the fully carbonaceous structure does not allow an easy chemical interaction between CFs and CNTs, different surface activation methods have been exploited to promote the formation of functional groups that could allow the two species to chemically bind [17]. The first attempts in promoting chemical bonding between the two species involved the functionalization of one species with carbonyl chloride groups and of the other one with amine ones, in order to form an amide linkage by nucleophilic substitution [18]. In order to simplify the process, a unique acid oxidation treatment was performed on both CFs and CNTs, then they were bound by coupling agents like dendrimers and PAMAM [19,20]. This approach avoids the double functionalization but leads to a lower grafting density due to the steric hindrance induced by the coupling agent [21]. More recent approaches are based on the oxidation of the carbon-based species followed by an esterification reaction, thus leading to higher grafting density [22,23]. In previous work by some of the authors, a simple and effective process to graft CNTs onto CFs was proposed [24]. In the present work, instead, the tape casting technique was employed to produce polyvinyl butyral (PVB) based composite tapes. CFs and CNTs were employed in different concentrations to assess their performance as reinforcement fillers. The multiscale composites were then produced by grafting CNTs onto the fibre surface, and compared with composites obtained by simple mixing of CFs and CNTs together in the PVB.

2. Specimen preparation

2.1 Materials

Carbon fibres were purchased from TOHO-Tenax; as reported by the manufacturer, the CFs are 6 mm long and sized with PU (polyurethane) up to 2.5% in weight, the bulk density is declared to be 530 g/dm^3. MultiWalled Carbon Nanotubes (MWCNTs) were acquired from Nanocyl, produced by catalytic chemical vapor deposition, and display the following characteristics: 9.5 nm average diameter, 1.5 µm average length, 90% purity and 250-300 m^2/g surface area, as stated by the producer. For the oxidation and grafting treatments, sulfuric acid (H_2SO_4) 98% v/v, nitric acid (HNO_3) 65% v/v, sodium hydroxide (NaOH) with 97% purity, and acetone with assay > 99.9% were used. All of the above-mentioned chemicals were purchased from Sigma Aldrich and matched the analytical standard specifications.

2.1 Oxidation of CFs and CNTs

For the oxidation of CFs, 2.0 g of CF were accurately weighted and placed in a 100 ml beaker. The acidic functionalization was performed by soaking the CFs in 80 ml sulfonitric acid solution (1 HNO_3 : 3 H_2SO_4) prepared by adding first 20 ml of nitric acid and then 60 ml to the beaker where CFs were placed. In order to promote the oxidation process the suspension was sonicated in an ultrasonic bath (SONICA 2400 MH series) for 30 minutes. At the end of the treatment, the solution was neutralized in a basic solution of 1 M NaOH until pH 7 was reached. Functionalized carbon fibres were then recovered via filtration with a fritted glass filter class G3 Pyrex. Fibres and CNTs were washed several times with distilled water and dried overnight in an oven at 80 °C. The same procedure was used to chemically oxidize 0.5 g of the CNTs; in this case, a filter with a fritted glass filter class G4 Pyrex was used.

2.3. Grafting.

For the grafting of CNTs on CFs, 0.2 g of the oxidized CFs were dispersed over a glass plate in order to maximize the contact area, while different quantities of the treated CNTs were dispersed in acetone using an ultrasonic probe (Vibra-cellTM) at 100 W power. The CNT dispersion was poured, drop-by-drop, over the carbon fibres waiting for the solvent to evaporate. To avoid the tendency of CNTs to aggregate in bundles and to maintain an effective dispersion, extra sonication steps were repeated in the ultrasonic bath for 5 minutes every 10 minutes. After all of the CNTs dispersion was poured over the CFs, the CF-CNT system was placed in an oven at 200 °C for 5 hours in order to promote chemical bonding, as suggested by Laachachi and coworkers [17]. After the thermal treatment, the CFs functionalized with CNTs were washed with pure water and dried in an oven at 60 °C. Different amounts of CNTs and CFs were used for the preparation of the various samples listed in Table 1. The acronym "G" is used to indicate the structure of the reinforcement obtained with the grafting procedure. Note that the labels used for the samples are related to the final CNT/CF reinforcement content in the composites, as discussed in the following paragraph.

Table 1: Sample labels and corresponding amounts of CNTs and CFs used for chemical grafted samples.

Sample	CF mass [g]	CNT mass [g]	CF/CNT mass ratio
G 0.5-0.25	0.3	0.15	2
G 0.5-0.17	0.3	0.1	3
G 0.5-0.1	0.2	0.04	5
G 0.5-0.025	0.2	0.01	20
G 0.5-0.01	0.2	0.004	50

2.4. Composite manufacturing by tape casting technology.

The slurry for tape casting was prepared by dispersing different fillers i.e. CFs, CNTs and grafted CFs in a solution of PVB in ethanol. An amount of 40 g of ethanol was weighed in a beaker, the same was done with 10 g of PVB; the fillers were then prepared in the required amounts and mixed with the ethanol; a small portion of PVB (0.6-0.8 g) was then added to the ethanol-based system, which was then mixed with a magnetic stirrer. When the solution became transparent, it was ultra-sonicated with an ultrasonic tip for 10 minutes with a power of 100 W. In the cases in which the dispersion was not sufficiently uniform, an additional sonication time of 5 minutes was necessary.

The aim of the ultrasounds treatment was to disperse the reinforcement, in particular CNTs, in the matrix. A small amount of PVB was added before the treatment in order to improve the dispersion and prevent the fillers from reaggregating in bundles at the end of ultrasound treatment.

The system was then placed on a magnetic stirrer that provided a mild but continuous agitation, and the remaining PVB added slowly (about 2 g/h). During the processing, the beaker was kept covered in order to prevent solvent evaporation. The solution was stirred overnight before being processed.

In Table 2, the different slurries prepared are listed; the filler fraction values are percentage by weight of the PVB, and are also used to define the nomenclature of the samples. We use the labels "NG" and "G" to indicate "Non-Grafted", and "Grafted" fibres, respectively.

After the stirring was completed, the slurry was degassed by mean of a vacuum pump in order to remove the air bubbles that would act as defects in the final composite. The resulting slurries were poured by tape casting on a movable mylar support (advance speed 100 mm/min); the doctor blade was adjusted to a height of 1 mm. By slow evaporation of the solvent, occurring at room temperature in air for 12 h, composite tapes with a thickness of 200–250 μm and without macroscopic defects were obtained.

Table 2: Sample labels and corresponding slurry composition.

Sample	CF weight fraction [%]	CNT weight fraction [%]
PVB	0	0
CF 0.1	0.1	0
CF 0.5	0.5	0
CF 1	1	0
CNT 0.025	0	0.025
CNT 0.1	0	0.1
CNT 0.5	0	0.5
CNT 1	0	1
NG CF 0.1 CNT 0.1	0.1	0.1
NG CF 0.5 CNT 0.01	0.5	0.01
NG CF 0.5 CNT 0.025	0.5	0.025
NG CF 0.5 CNT 0.1	0.5	0.1
NG CF 1 CNT 0.1	1	0.1
G CF 0.5 CNT 0.01	0.5	0.01
G CF 0.5 CNT 0.025	0.5	0.025
G CF 0.5 CNT 0.1	0.5	0.1

3. Results and discussion

3.1 Thermal analysis

The thermal behaviour of CNTs, pure CFs and grafted CFs was studied by thermogravimetric analysis (TGA). The samples were prepared by accurately cleaning each material and then drying it in an oven at 80 °C. The TGA analysis was performed in flowing air at 50 ml/min, with a heating ramp of 10 °C/min up to 1000 °C.
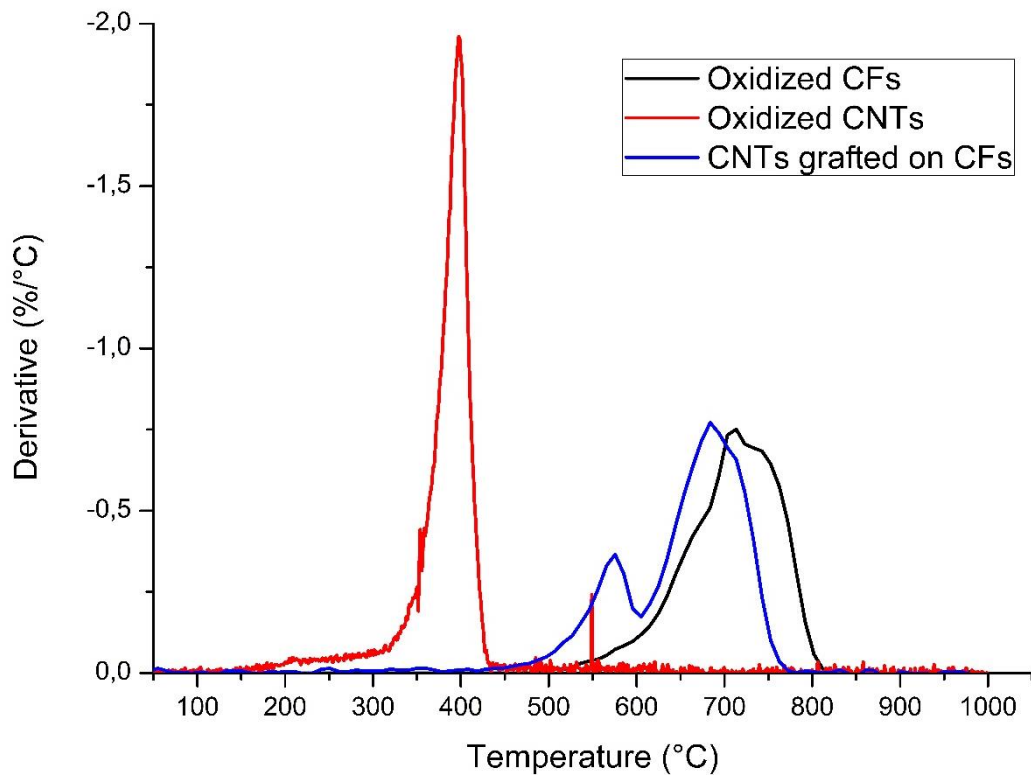
Fig. 1*: TGA derivative curves of oxidized CFs and CNTs (with sulfonitric acid) compared with grafted CFs (CF/CNT ratio equal to 20)*

The TGA curves show how the degradation of the three samples starts at different temperatures. The grafted CF samples follow a curve that lies between that of oxidized CF samples and that of CNT samples, as expected. Moreover, while CF and CNT samples present a unique peak in the derivative curves, a different behaviour is observed for the grafted CNTs, for which two peaks can be observed. This suggests that the degradation proceeds through two steps: first the degradation of CNTs and subsequently degradation of the CFs. It can be also noted how in the grafted fibres the thermal degradation of CNTs starts at a much higher temperature than the oxidized CNTs. This phenomenon is probably due to the absence of oxygen-containing groups, which are no longer present on the CNTs surface since they were used in the esterification reaction to form chemical bonds with the CFs. Since such groups begin their degradation at lower temperature, in their absence the overall degradation starts at higher temperature.

3.2. Surface morphology

The surface morphology of the samples was observed by means of a Zeiss Merlin Field Emission Scanning Electron Microscope (FESEM). Samples were prepared for each grafted-fibre batch. Various images were taken at different magnifications and in different areas of the samples in order to observe representative samples of the morphology of the grafted fibres for different CNT

contents. In Figure 2, the G CF 0.5 CNT 0.01 sample is observed at increasing magnifications. As can be seen in Fig. 2a, it appears that the CNTs do not extend over the whole surface of the CFs. This non-uniform surface covering can be attributed to the small amount of CNTs used in the grafting treatment for this specific sample, which did not allow the entire CF surface to come in contact with the CNTs. The same behaviour is observed in the case of the G CF 0.5 CNT 0.025 sample. Moreover, it is possible to notice the presence of large CNT aggregates on the CF surface, which could be due to the use of acetone to promote the reaction between CFs and CNTs, since this solvent is not effective for keeping the CNTs well dispersed. Larger magnification on single CFs (Figs.2b, 2c and 2d) highlights the presence of a relatively uniform layer of CNTs, with the nanotubes lying mainly parallel to the fibre surface.
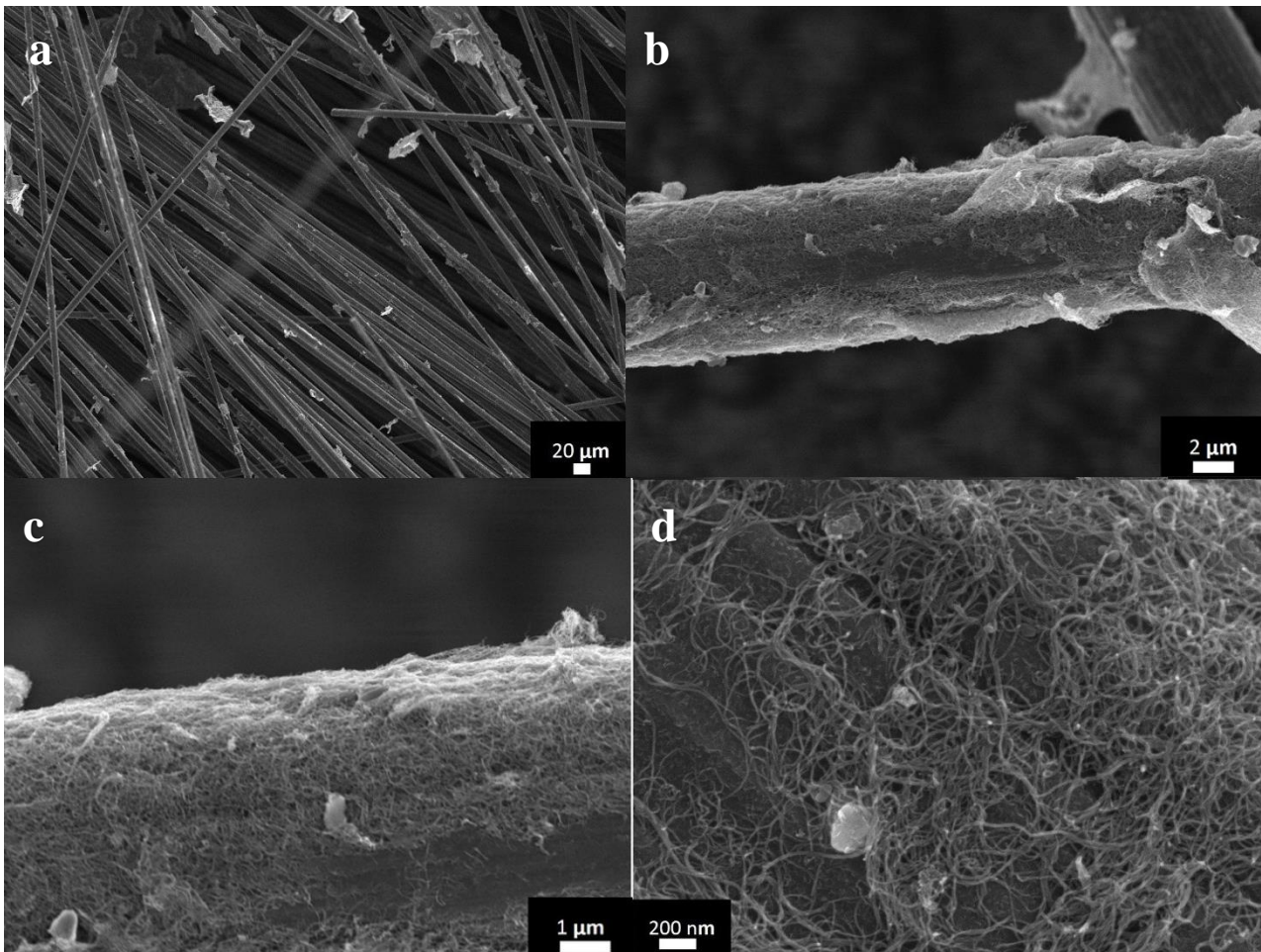

Fig. 2*: SEM images of the CF surface in a G CF 0.5 CNT 0.01 sample at different magnifications: a) 2500 X b) 10000 X c) 25000 X d) 200000 X.*

In the case of G CF 0.5 CNT 0.01 samples, a considerable morphological change is observed, since CFs become uniformly covered by nanoscale spherical particles (Fig. 3). These particles display a

spherical geometry with a diameter ranging approximately from 20 nm to 250 nm. Some holes are present on the fibre surface. This suggests that the nanospheres can be identified as Carbon Nano Onions (CNOs) [24,25]. The CNO spheroidal structures can be synthetized from CFs, since the strong acid treatment probably weakens the bonds between differently-oriented carbon structures in the fibres, and CNOs emerge out of the surface of the CFs from the liquid phase during the grafting process [26]. It must also be noted that the CNTs appear to interact with the CNOs. In particular, CNTs seem to act as nanometric ropes that keep the onions bound to the fibres, although this requires a rather high CNT concentration. Further studies will be required to define the range of conditions under which it is possible to obtain this specific morphology, however the possibility of improving the roughness of the carbon fibres with a strong interfacial layer made of CNOs/CNTs is thought to be extremely beneficial for the mechanical properties of composites, as discussed below.
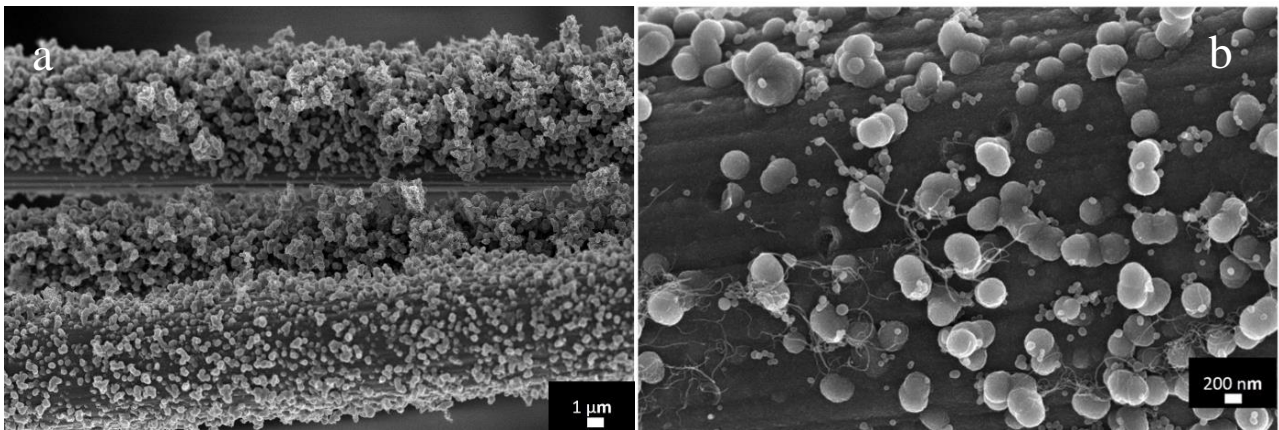

Fig. 3: SEM images of a G CF 0.5 CNT 0.1 sample at different magnifications: a) 10000 X b) 50000 X

3.3 Mechanical testing

Tensile tests were performed on the samples using a ZwickLine z050 testing machine with a 50 kN load cell. The test was conducted at room temperature in displacement control at a velocity of 0.5 mm/min and applying a preload of 5 N. All measurements were also subsequently repeated and verified using a universal testing machine MIDI 10 by Messphysik Materials Testing, at a velocity of 0.6 mm/min, corresponding to a strain rate of about $0.025\%s^{-1}$. The samples were rectangular specimens, cut from the fabricated tapes, 57 x 9 or 40 x 9 mm^2 in size with variable thickness, as reported in Table 3. The unreinforced polymer is indicated with "PVB", while the thickness variation among the samples depends on the viscosity of the slurry before casting and on the rate of

solvent evaporation, thus on the quantity of CNTs or CF present in the composites. For most of the samples, a thickness of approximately 100 μm was obtained. Adhesive pads were glued on the specimen ends in order to fit the testing machine grips and avoid slippage during loading. The tests allowed to determine stress-strain curves for the various specimens in the quasistatic regime, and to derive the quantities of interest such as stiffness, yield stress, strength, ultimate strain.

Table 3: Geometrical dimension of the specimens.

Sample label	Length [mm]	Width [mm]	Thickness [mm]	Section [mm^2]
PVB	57 (40)	9	0.04	0.32
CF 0.1	57 (40)	9	0.05	0.45
CF 0.5	57 (40)	9	0.09	0.81
CF 1	57 (40)	9	0.09	0.81
CNT 0.025	57 (40)	9	0.10	0.90
CNT 0.1	57 (40)	9	0.11	0.95
CNT 0.5	57 (40)	9	0.10	0.90
CNT 1	57 (40)	9	0.10	0.90
NG CF 0.1 CNT 0.1	57 (40)	9	0.09	0.77
NG CF 0.5 CNT 0.1	57 (40)	9	0.11	0.99
NG CF 0.5 CNT 0.025	57 (40)	9	0.10	0.9
NG CF 0.5 CNT 0.01	57 (40)	9	0.09	0.81
NG CF 1 CNT 0.1	57 (40)	9	0.09	0.81
G CF 0.5 CNT 0.1	57 (40)	9	0.08	0.72
G CF 0.5 CNT 0.025	57 (40)	9	0.09	0.81

The tests were performed on every composite by loading up to failure several specimens (from 5 to 16) for each type. The onset of damage occurs typically at both sides of the tape, followed by specimen tearing which induces torsion. Some examples of fractured specimens are shown in Fig. 5.

In order to observe how the addition of CFs and CNTs affects the mechanical behaviour, in the following a comparison will be provided for the different families of composites produced.
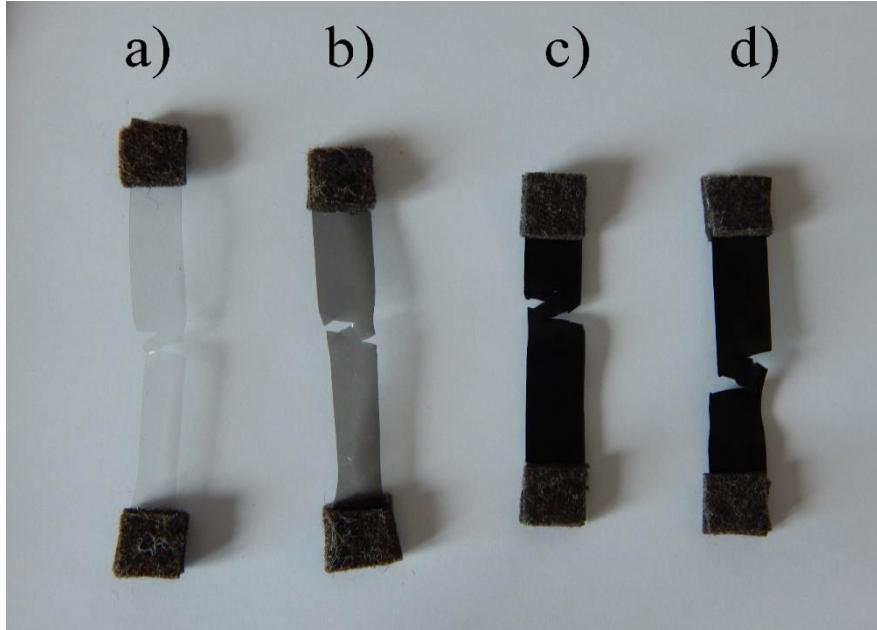
Fig 4: *Fractured specimens of different types: a) CNT 0.025 b) CNT 0.1 c) CNT 0.5 d) CNT 1*

3.3.1. CF and CNT-reinforced composites.

A typical stress-strain curve for various samples is shown in Fig. 5. It is apparent that the addition of CFs leads to a 30% increase in strength and promotes brittle fracture. The further addition of CNTs provides a small additional increase in strength, but also a considerable toughening of the composite, with a transition from brittle to ductile fracture, an increase in the ultimate strain, and the corresponding increase of over 10 times in the dissipated energy, per unit mass *E/m*. The latter is taken as a measure of material toughness and is calculated as:

$$\frac{E}{m} = \frac{1}{\rho} \int_0^{\varepsilon_f} \sigma d\varepsilon \qquad (1)$$

where σ is the stress, ε the strain, ρ the material density, and ε_f the ultimate strain [27]. Large simultaneous strength and toughness values are distinctive of biological materials, which can conjugate these two mutually exclusive properties through hierarchical structures and multiscale damage mechanisms [28]. Therefore, these are extremely important properties to be achieved in the development of bioinspired materials.
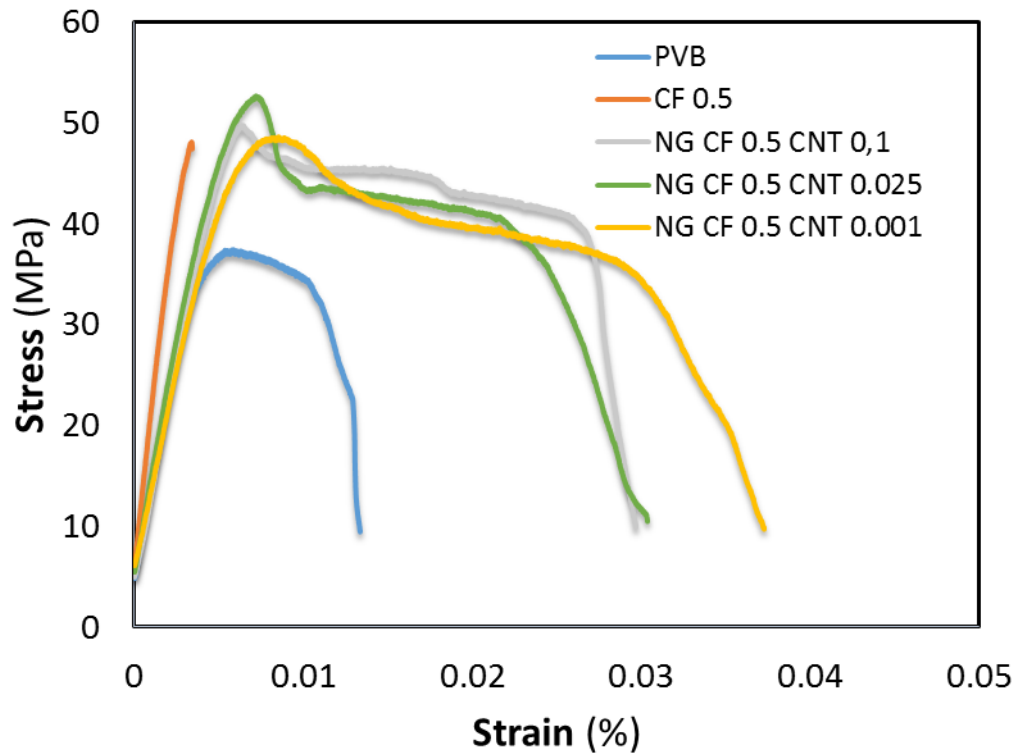
Fig 5: Examples of stress vs. strain for different CF/CNT reinforced PVB composites.

To evaluate the reinforcing effect of CFs and CNTs separately, average mechanical properties of (non-hierarchical) composites with only a single reinforcement type (CFs or CNTs) are initially analysed (Fig. 6 and Table 4). Predictions using a direct and inverse Rule of Mixtures (RM) are included as lines in the plots for comparison [29], using the data in Table 5 for the matrix and fibre properties.
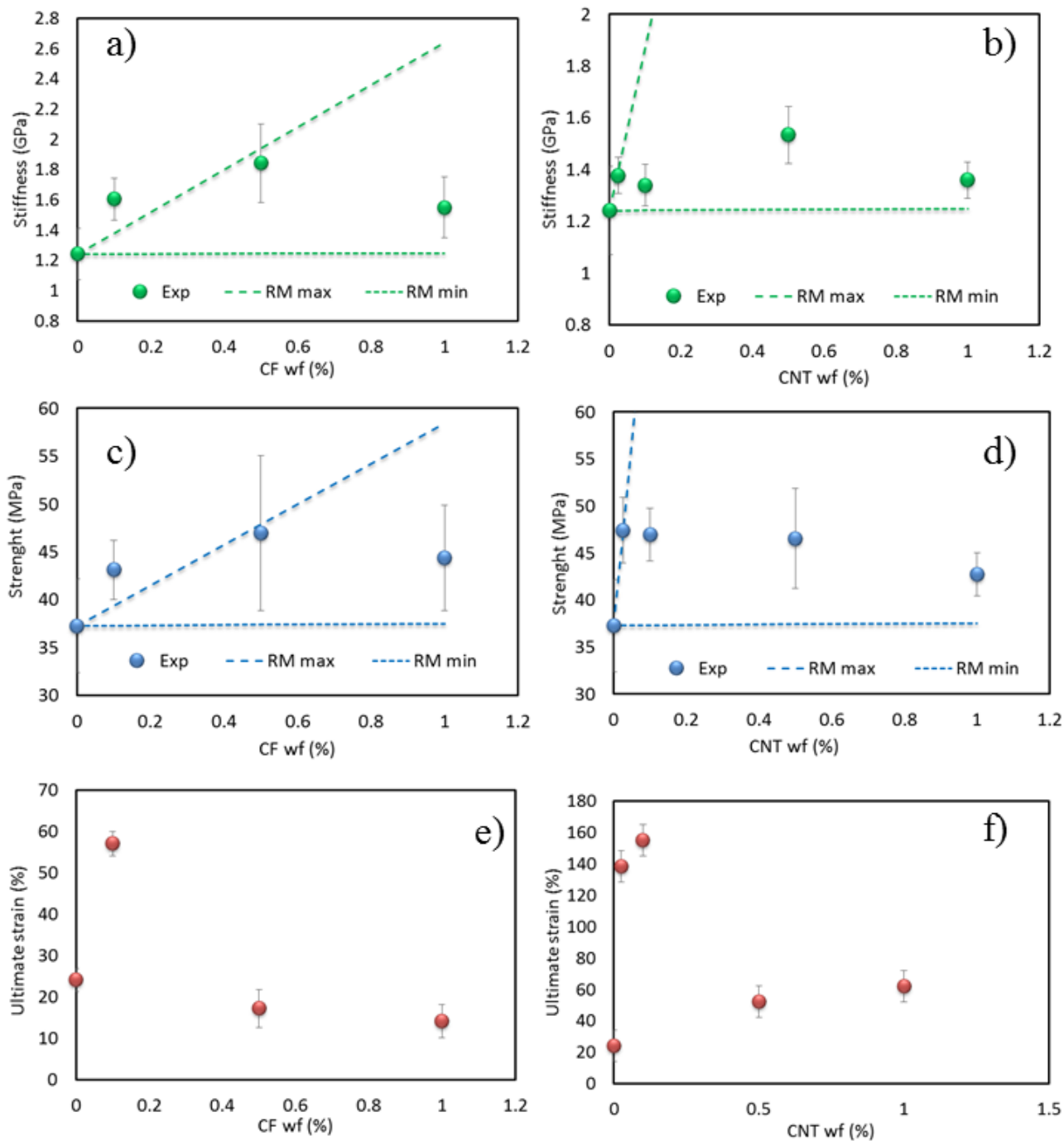
Fig 6: *Average stiffness, strength, and ultimate strain values for CF-reinforced PVB (left column) and CNT-reinforced PVB (right column) composites. Dotted lines display direct ("RM max") and inverse ("RM min") rule of mixtures predictions*

Table 4: *Average mechanical properties of CF and CNT composite tapes measured in tensile testing.*

Sample	Stiffness (GPa)	Strength (MPa)	Ultimate Strain (%)	Toughness (J/g)
PVB	1.2±0.2	37.3±4.9	24.2±2.8	150±36
CF 0.1	1.8±0.1	43.1±3.1	57.1±1.4	122±14
CF 0.5	1.6±0.1	46.9±8.1	17.2±4.6	92±32
CF 1	1.4±0.1	44.4±5.5	14.1±5.3	135±40
CNT 0.025	1.4±0.1	47.4±3.5	138.4±1.1	222±47
CNT 0.1	1.2±0.1	47.0±2.8	154.9±2.5	164±16
CNT 0.5	1.5±0.1	46.6±5.3	52.2±4.7	146±49
CNT 1	1.6±0.2	42.7±2.3	61.9±10.3	139±15

Results show that the composites reinforced with CFs achieve an increase in stiffness and strength with increasing CF weight fraction, up to a maximum for 0.5% CFs. This increase is consistent with RM predictions, indicating that the fibres are well aligned. For larger fibre contents, the effects of imperfect dispersion become non negligible, since the CFs agglomerate in bundles that behave as brittle inclusions, leading to a decrease in the overall strength of the composites. The ultimate strain increases with respect to pure PVB in the case of the sample containing 0.1% CFs while at 0.5% CFs the fracture becomes brittle. This effect is again related to the size of the reinforcements: for 0.1% CFs there is sufficient space between the fibres to guarantee the deformation of the samples, while in the case of a higher CF content, the effect of local stiffening of the polymer induced by the fibres prevails and fracture becomes brittle. There is good reproducibility in the measured stiffness and strength values, while ultimate strain and therefore toughness values are subject to a greater variability. This is mainly related to the onset of torsional or misalignment effects occurring in the tape specimens once damage sets in, as can be observed for some of the damaged specimens in Fig.4. The misalignment effects are dependent on the type and location of damage in the specimen, and thus lead to an increase in the standard deviation of ultimate strain and toughness values.

Table 5: *Material properties used in direct and inverse RM*

Property	PVB	CF	CNT
Density (kg/m^3)	1070	1760	1350
Young's modulus (GPa)	1.24	230	800
Strength (MPa)	37.3	3500	50000

SEM analysis of fracture surfaces of CF-reinforced samples (Fig. 6) shows that as expected fibres are mainly oriented along the tape direction due to the shear stresses acting during the tape casting process. Partial debonding and pull-out from the matrix is observed (Fig. 6). This suggests a relatively weak interface between the polymer and the fibres, which leads to limited toughness values, consistently with observed ultimate strain values.
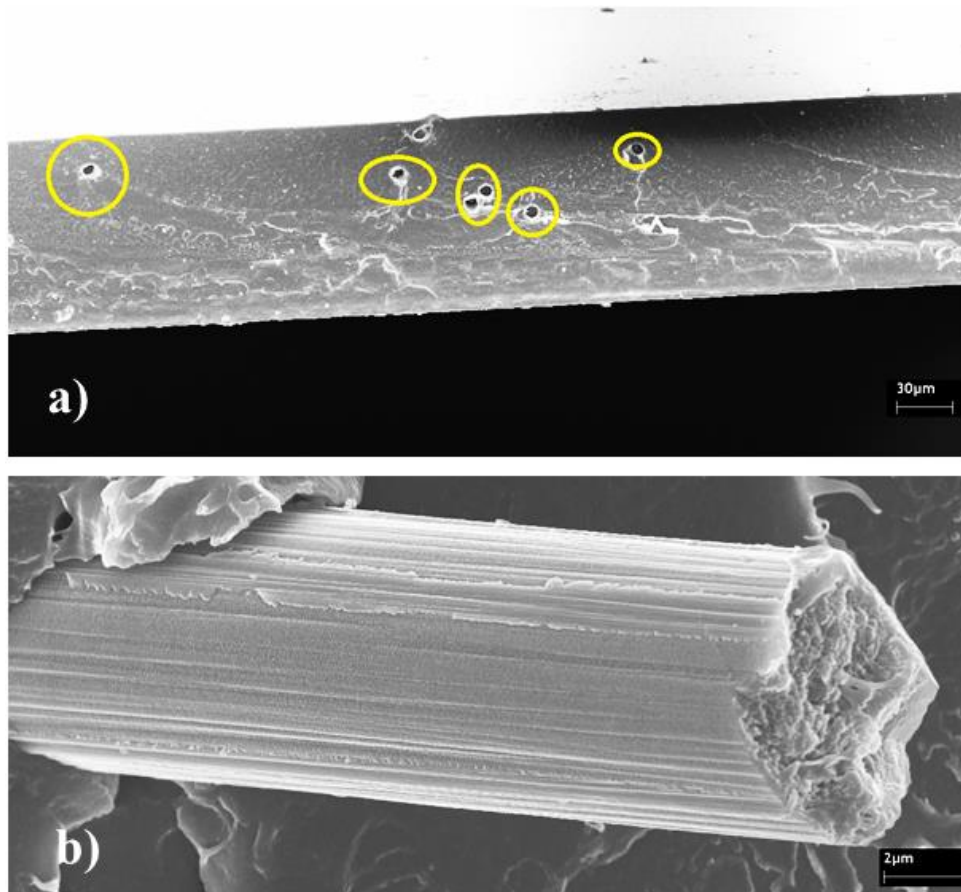

Fig 6: SEM image of a CF 0.5 sample at (a) 700X magnification (b) 15000X magnification, highlighting fibre pull-out.

The stiffness and strength data indicate that 0.5% is the optimal CF weight fraction to provide the best mechanical properties. This is because this concentration allows a good dispersion of CFs during composite manufacturing with limited fibre aggregation. Analysis of the fracture surfaces suggests that an improvement in the interface could significantly change the mode of fracture of these composites, and lead to further toughness improvements.

The addition of CNTs also significantly improves mechanical properties in terms of stiffness and tensile strength, as expected. However, the best mechanical performance, comparable with RM

predictions, is obtained at a very low weight fractions (0.025% wf for tensile strength and 0.1% wf for ultimate strain), while higher percentages lead to a degradation of the mechanical properties, with properties considerably below direct RM predictions. This is due to the fact that low CNT concentrations allow a uniform dispersion of the filler in the matrix and a better exploitation of the exceptional mechanical properties of the single CNTs. When the CNT concentration is increased, nanotube bundles tend to form behaving as structural defects, counterbalancing the positive effect of the increased CNT concentration in the matrix (Fig. 7). The smaller amount of filler needed to reach the optimal stiffness and strength with respect to the case of CF-reinforced composites is related to the higher CNT stiffness and strength values, making them more effective in providing reinforcement effects at lower weight fractions. In addition, some nanoscale-related effects can occur, leading to a change in the local properties of the polymer matrix due to the high CNT surface area and the vicinity between CNTs even at low weight fractions. Additionally, CNTs can potentially interact with surrounding polymer chains and modify the crystalline morphology of the matrix [30].
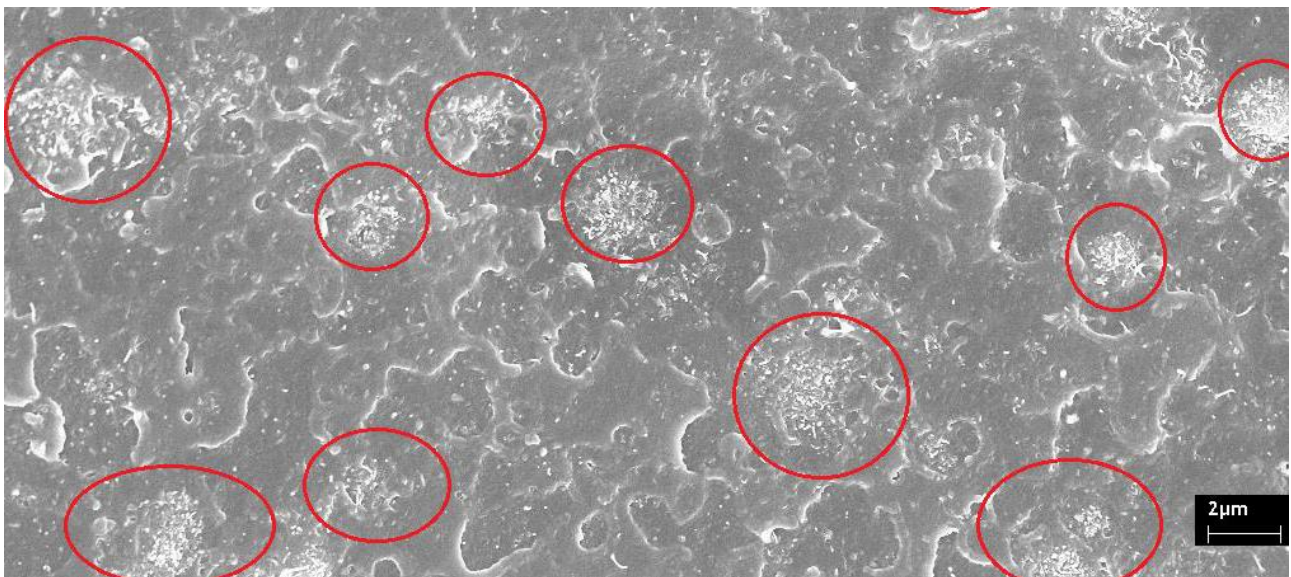

Fig 7: SEM image of a CNT 1 sample at 10000X magnification. Red circles indicate CNT agglomeration in bundles.

The latter effects are responsible for the observed increase in ultimate strain for CNT-reinforced samples, leading to a higher toughness composite. Necking and unfolding of polymer chains is improved by the addition of a small amount of CNTs, while it is hindered by the presence of CNT agglomerates. In the case of PVB-CNTs composites, a chain-wrapping phenomenon is hypothesized at the interface between CNTs and PVB [31]. When a tensile stress is applied, the

chains start to unfold, sliding along the nanotubes, giving rise to an improved elongation at break with respect to the pure polymer.

3.3.2. Multiscale composites

To evaluate the influence of multiscale hierarchical structure on the mechanical behaviour of the considered CF-CNT composites, a comparison is made between samples with CNTs grafted on the CF surfaces ("G" samples), and samples where the CFs and CNTs are simply mixed in the matrix ("NG" samples"). The measured stiffness and strength values for the same CF and CNT content for the two types of composite are reported in Fig. 8 and in Table 6. As discussed in the previous section, the CF weight fraction for which best results are obtained in the case of a single-reinforcement composite is kept constant (0.5 %) and CNT content varies between 0.01 % and 0.1%. Results show an improvement in both stiffness and strength of the composites containing both CFs and CNTs with respect to the case of the composites with only single reinforcement types (Fig.6). A further improvement is observed in the case of "G" samples compared to "NG" samples. In the best case, a stiffness and strength increase of 45% and 47% is obtained compared to PVB, of 18% and 23% compared to the CF 0.5 specimens, and of 24% and 28% compared to the non-grafted CNT case. Writing the direct RM for strength as:

$$\sigma_{CF} = \frac{\sigma_C - \sigma_{PVB}(1 - f_{CF})}{f_{CF}} \qquad (2)$$

where σ_{CF} is the CF strength, σ_C is the composite strength, σ_{PVB} is the matrix strength, and f_{CF} the CF volume fraction, one can derive that the effect of adding grafted CNTs is equivalent to using CFs that are twice as strong as conventional ones (7.7 GPa instead of 3.5 GPa).

Table 6: *Average mechanical properties of multiscale (grafted: "G") and conventional (non-grafted: "NG") CF/CNT composite tapes measured in tensile testing.*

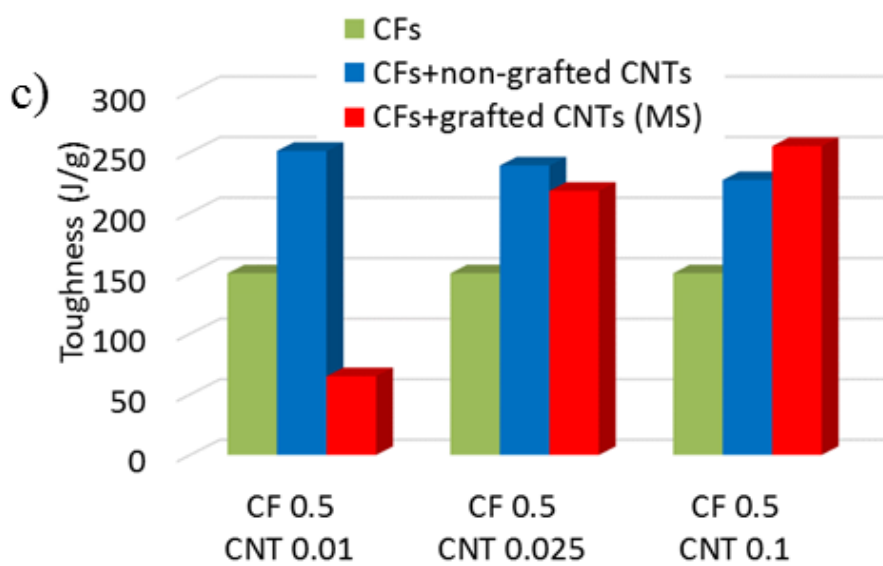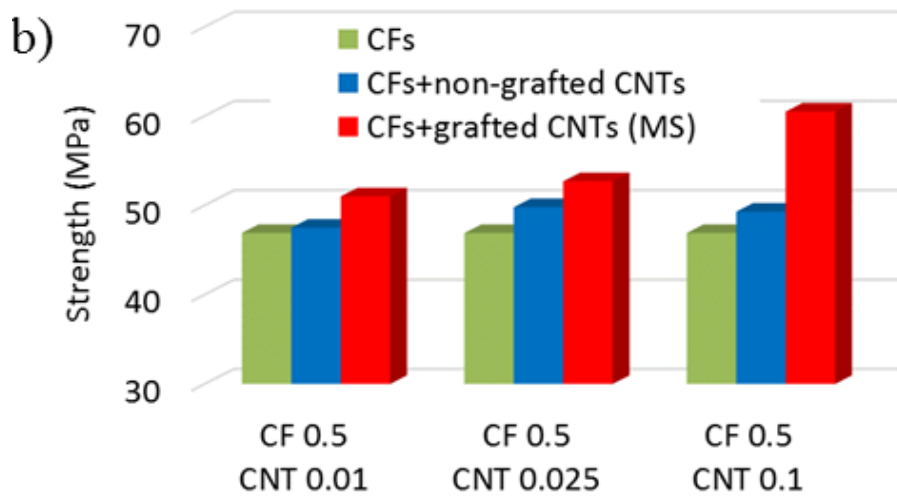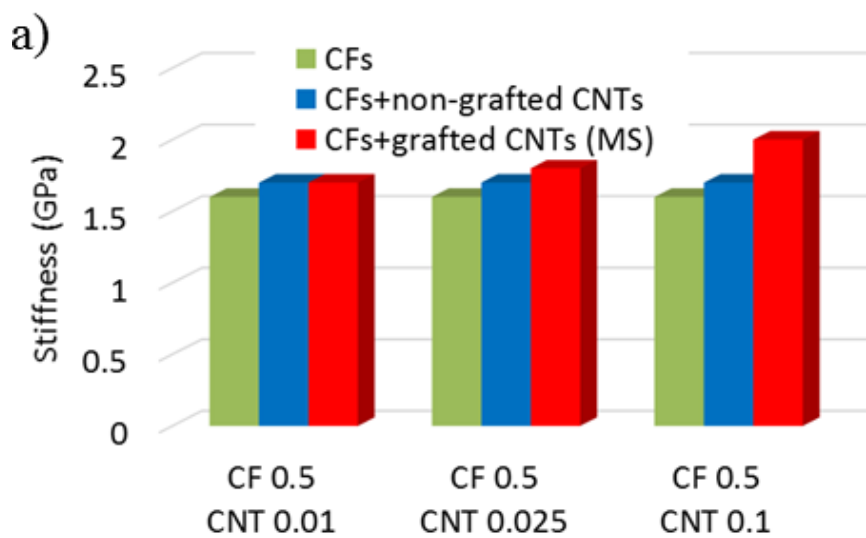| Sample	Stiffness (GPa)	Strength (MPa)	Ultimate Strain (%)	Toughness (J/g)
NG CF 0.5 CNT 0.01	1.7±0.1	47.5±1.2	29.6±15.5	251±51
NG CF 0.5 CNT 0.025	1.7±0.1	49.8±1.8	27.5±11.6	239±49
NG CF 0.5 CNT 0.1	1.7±0.1	49.3±3.9	31.6±23.9	227±53
G CF 0.5 CNT 0.01	1.6±0.3	51.0±3.4	3.2±0.69	65±28
G CF 0.5 CNT 0.025	1.8±0.1	52.7±6.0	35.6±18.7	218±23
G CF 0.5 CNT 0.1	2.0±0.1	60.5±0.2	19.9±7.1	255±18

a)

b)

c)

Fig. 8: Stiffness, strength and toughness of multiscale (MS) composites with CNTs grafted on CFs compared with composites with non-grafted CNTs and with conventional CF composites. The MS composites optimize both strength and toughness.

This behaviour is due to the hierarchical structure of the reinforcements in "G" samples shown in Fig.2 and Fig.3, which enhances the adhesion between fibre and matrix, giving rise to a strength increase. Moreover, a stronger interface between fibres and matrix allows the sliding of the polymer chains during damage evolution within the polymer itself, rather than at the interface with the carbon fibres (one could also speak of "interphase" rather than "interface", since it is the presence of an additional phase, i.e. CNTs, that modifies the interaction between polymer and the reinforcing fibres). Thus, the overall fracture process becomes more ductile, with greater polymer deformation around the fibre rather than fibre pull-out from of the polymer. This leads to a simultaneously stronger and tougher material.

On the other hand, the properties of the mixed composites with non-grafted fibres lie between those of multiscale ones and single-fibre reinforced ones. The CNT content does not significantly alter the mechanical properties of CF 0.5 samples, confirming the indication that a good dispersion of CNTs is obtained for small weight fraction values, while agglomeration effects take place at greater concentrations. Consistently with previous observations, in most cases samples containing small amounts of CNTs show plasticization effects that lead to larger ultimate strain value and toughness.

4 Numerical analysis of CF-CNT interface properties

The improvement in mechanical properties identified in specimens with grafted CNTs discussed in the previous sections is attributed to the improvement in interface properties between CFs and matrix, which helps prevent fibre pull out during specimen failure. This improvement can be highlighted by analysing stress distributions at the interface for CFs with and without grafted CNTs. In particular, we qualitatively evaluate the distributions in the case of the presence of CNOs (Fig. 3) by means Finite Element (FE) simulations using COMSOL Multiphysics. An axisymmetric model of a single CF embedded in a PVB matrix with and without grafted CNOs is considered. The fibre is 50 μm in length and CNOs (200 nm in radius) are regularly spaced at 2 μm along its length. Material properties are taken from Table 5. Figure 9 shows the shear stress concentrations in and around the embedded matrix when a unit pull-out force P is applied to the fibre end. The corresponding stresses at the interface highlight the mechanism responsible for the improvement of interface properties for hierarchical fibres. In the case of a non-grafted fibre, the stress peaks occur

at the fibre ends, giving rise to anticipated fibre-matrix debonding and fibre pull-out. Instead, the presence of CNOs along the fibre give rise to a redistribution of stresses, and a reduction in the stress peaks, thus leading to a greater load bearing capacity and improved overall composite strength, as observed experimentally.
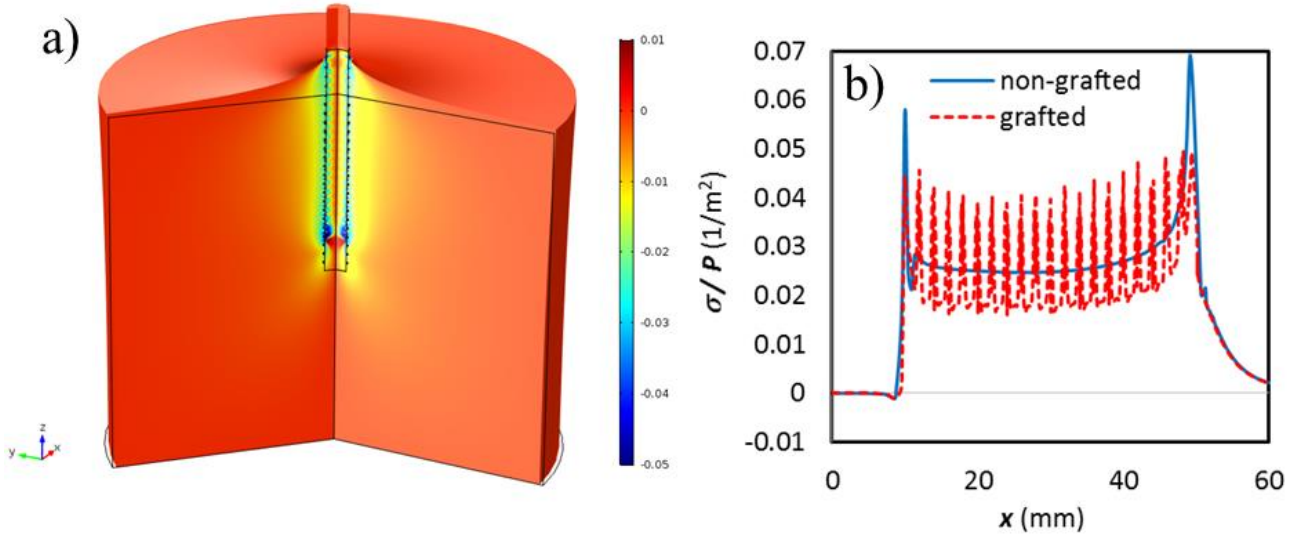

Fig. 9: FE results of the pull-out from a PVB matrix of a CF with grafted CNOs: a) Stress σ (per unit pull-out load P) distribution in the matrix and fibre; b) Calculated stresses at the interface for grafted and non-grafted fibres.

The increase in toughness between a CF-reinforced composite and a MS composite can be quantified using a recently-introduced "hierarchical shear lag" theory by some of the authors [32], according to which the increase of dissipated energy during fibre pull-out per unit contact area W_2/A_2 when adding a hierarchical level to a fibrillar system can be expressed as:

$$\frac{W_2}{A_2} = \frac{W_1}{A_1}\left(2 + \frac{l_d}{l_a}\right) \tag{3}$$

where W_1/A_1 is the dissipated energy per unit area for the non-hierarchical system, l_d is the average detached length of second-level fibrils (CNTs in this case) and l_a their attached length. Thus, the additional hierarchical level produces at least a doubling of toughness, which is compatible with the observed values, at least for sufficient CNT concentrations to ensure uniform coating of the CF. The l_a value is also inversely proportional to the linear density of grafted CNTs on the CF, so Eq.(3)

correctly predicts an increase in toughness with increasing CNT concentration, at least until self-bunching effects set in.

Conclusions

In conclusion, our experimental results on CF/CNT reinforced PVB composite tapes show that it is possible to obtain a considerable increase in stiffness, strength and toughness with respect to the pure polymer by using relatively low reinforcement weight fractions. The addition of single fillers (either CFs or CNTs) leads to increments of up to 50% in stiffness, 30% in strength, and up to 500% in ultimate strain. Larger weight fractions lead to saturation effects given by dispersion difficulties. The mixture of CFs and CNTs produces a further improvement that can be ascribed to a synergic interaction of the two different fillers. The best results, however, are obtained when a hierarchical bioinspired structure is attained using surface-grafted CNTs on CF reinforcing fibres, since fibre-matrix interface properties are significantly improved and fibre pull-out effects are reduced, leading to a further 60% increase in stiffness and 20% increase in strength with respect to the non-hierarchical case. Morphological analysis and numerical simulations support the interpretation of the role of the grafted CNTs on the mechanical performance. These results provide useful indications for the manufacture of stronger and tougher polymer nanocomposites and could contribute in fully realizing the potential of nanocomposites in the field of advanced materials using the concepts provided a bioinspired approach.

References

[1] M. Bhattacharya, Polymer Nanocomposites—A Comparison between Carbon Nanotubes, Graphene, and Clay as Nanofillers, Materials. 9 (2016) 262. doi:10.3390/ma9040262.

[2] J.N. Coleman, U. Khan, W.J. Blau, Y.K. Gun'ko, Small but strong: A review of the mechanical properties of carbon nanotube–polymer composites, Carbon. 44 (2006) 1624–1652. doi:10.1016/j.carbon.2006.02.038.

[3] H. Gao, B. Ji, I.L. Jager, E. Arzt, P. Fratzl, Materials become insensitive to flaws at nanoscale: Lessons from nature, Proc. Natl. Acad. Sci. 100 (2003) 5597–5600. doi:10.1073/pnas.0631609100.

[4]   J. Aizenberg, Skeleton of Euplectella sp.: Structural Hierarchy from the Nanoscale to the Macroscale, Science. 309 (2005) 275–278. doi:10.1126/science.1112255.

[5]   J.-Y. Rho, L. Kuhn-Spearing, P. Zioupos, Mechanical properties and the hierarchical structure of bone, Med. Eng. Phys. 20 (1998) 92–102.

[6]   C. Zhang, D.A. Mcadams, J.C. Grunlan, Nano/Micro-Manufacturing of Bioinspired Materials: a Review of Methods to Mimic Natural Structures, Adv. Mater. 28 (2016) 6292–6321. doi:10.1002/adma.201505555.

[7]   H. Qian, E.S. Greenhalgh, M.S.P. Shaffer, A. Bismarck, Carbon nanotube-based hierarchical composites: a review, J. Mater. Chem. 20 (2010) 4751. doi:10.1039/c000041h.

[8]   Y.C. Jung, B. Bhushan, Mechanically Durable Carbon Nanotube−Composite Hierarchical Structures with Superhydrophobicity, Self-Cleaning, and Low-Drag, ACS Nano. 3 (2009) 4155–4163. doi:10.1021/nn901509r.

[9]   D. Yu, K. Goh, H. Wang, L. Wei, W. Jiang, Q. Zhang, L. Dai, Y. Chen, Scalable synthesis of hierarchically structured carbon nanotube–graphene fibres for capacitive energy storage, Nat. Nanotechnol. 9 (2014) 555–562. doi:10.1038/nnano.2014.93.

[10]   H. Qian, A. Bismarck, E.S. Greenhalgh, G. Kalinka, M.S.P. Shaffer, Hierarchical Composites Reinforced with Carbon Nanotube Grafted Fibers: The Potential Assessed at the Single Fiber Level, Chem. Mater. 20 (2008) 1862–1869. doi:10.1021/cm702782j.

[11]   T. Yokozeki, Y. Iwahori, S. Ishiwata, K. Enomoto, Mechanical properties of CFRP laminates manufactured from unidirectional prepregs using CSCNT-dispersed epoxy, Compos. Part Appl. Sci. Manuf. 38 (2007) 2121–2130. doi:10.1016/j.compositesa.2007.07.002.

[12]   F.H. Gojny, M.H.G. Wichmann, B. Fiedler, W. Bauhofer, K. Schulte, Influence of nano-modification on the mechanical and electrical properties of conventional fibre-reinforced composites, Compos. Part Appl. Sci. Manuf. 36 (2005) 1525–1535. doi:10.1016/j.compositesa.2005.02.007.

[13]   Y. Iwahori, S. Ishiwata, T. Sumizawa, T. Ishikawa, Mechanical properties improvements in two-phase and three-phase composites using carbon nano-fiber dispersed resin, Compos. Part Appl. Sci. Manuf. 36 (2005) 1430–1439. doi:10.1016/j.compositesa.2004.11.017.

[14]   Y. Zhou, F. Pervin, L. Lewis, S. Jeelani, Experimental study on the thermal and mechanical properties of multi-walled carbon nanotube-reinforced epoxy, Mater. Sci. Eng. A. 452–453 (2007) 657–664. doi:10.1016/j.msea.2006.11.066.

[15]   A. Vivet, B.B. Doudou, C. Poilâne, J. Chen, M. Ayachi, A method for the chemical anchoring of carbon nanotubes onto carbon fibre and its impact on the strength of carbon fibre composites, J. Mater. Sci. 46 (2011) 1322–1327. doi:10.1007/s10853-010-4919-0.

[16] H. Rong, K.-H. Dahmen, H. Garmestani, M. Yu, K.I. Jacob, Comparison of chemical vapor deposition and chemical grafting for improving the mechanical properties of carbon fiber/epoxy composites with multi-wall carbon nanotubes, J. Mater. Sci. 48 (2013) 4834–4842. doi:10.1007/s10853-012-7119-2.

[17] A. Laachachi, A. Vivet, G. Nouet, B. Ben Doudou, C. Poilâne, J. Chen, J. Bo bai, M. Ayachi, A chemical method to graft carbon nanotubes onto a carbon fiber, Mater. Lett. 62 (2008) 394–397. doi:10.1016/j.matlet.2007.05.044.

[18] X. He, F. Zhang, R. Wang, W. Liu, Preparation of a carbon nanotube/carbon fiber multi-scale reinforcement by grafting multi-walled carbon nanotubes onto the fibers, Carbon. 45 (2007) 2559–2563. doi:10.1016/j.carbon.2007.08.018.

[19] L. Mei, X. He, Y. Li, R. Wang, C. Wang, Q. Peng, Grafting carbon nanotubes onto carbon fiber by use of dendrimers, Mater. Lett. 64 (2010) 2505–2508. doi:10.1016/j.matlet.2010.07.056.

[20] Q. Peng, X. He, Y. Li, C. Wang, R. Wang, P. Hu, Y. Yan, T. Sritharan, Chemically and uniformly grafting carbon nanotubes onto carbon fibers by poly(amidoamine) for enhancing interfacial strength in carbon fiber composites, J. Mater. Chem. 22 (2012) 5928. doi:10.1039/c2jm16723a.

[21] M.S. Islam, Y. Deng, L. Tong, S.N. Faisal, A.K. Roy, A.I. Minett, V.G. Gomes, Grafting carbon nanotubes directly onto carbon fibers for superior mechanical stability: Towards next generation aerospace composites and energy storage applications, Carbon. 96 (2016) 701–710. doi:10.1016/j.carbon.2015.10.002.

[22] G. Socrates, Infrared and Raman characteristic group frequencies: tables and charts, 3. ed., as paperback, Wiley, Chichester, 2010.

[23] K. Tsirka, G. Foteinidis, K. Dimos, L. Tzounis, D. Gournis, A.S. Paipetis, Production of hierarchical all graphitic structures: A systematic study, J. Colloid Interface Sci. 487 (2017) 444–457. doi:10.1016/j.jcis.2016.10.075.

[24] L. Lavagna, D. Massella, M. Pavese, Preparation of hierarchical material by chemical grafting of carbon nanotubes onto carbon fibers, Diam. Relat. Mater. 80 (2017) 118–124. doi:10.1016/j.diamond.2017.10.013.

[25] M. Zeiger, N. Jäckel, V.N. Mochalin, V. Presser, Review: carbon onions for electrochemical energy storage, J Mater Chem A. 4 (2016) 3172–3196. doi:10.1039/C5TA08295A.

[26] J.-C. Fan, H.-H. Sung, C.-R. Lin, M.-H. Lai, The production of onion-like carbon nanoparticles by heating carbon in a liquid alcohol, J. Mater. Chem. 22 (2012) 9794. doi:10.1039/c2jm13273g.

[27] S.P. Timoshenko, Strength of materials : part II, advanced., Van Nostrand Reinhold, New York, 1956.

[28] U.G.K. Wegst, H. Bai, E. Saiz, A.P. Tomsia, R.O. Ritchie, Bioinspired structural materials, Nat. Mater. 14 (2014) 23–36. doi:10.1038/nmat4089.

[29] M. Alger, Polymer Science Dictionary, 2nd ed., Springer Netherlands, 1997. 10.1007/978-94-024-0893-5.

[30] D.R. Paul, L.M. Robeson, Polymer nanotechnology: Nanocomposites, Polymer. 49 (2008) 3187–3204. doi:10.1016/j.polymer.2008.04.017.

[31] M. Yang, V. Koutsos, M. Zaiser, Interactions between Polymers and Carbon Nanotubes: A Molecular Dynamics Study, J. Phys. Chem. B. 109 (2005) 10009–10014. doi:10.1021/jp0442403.

[32] L. Brely, F. Bosia, N.M. Pugno, Emergence of the interplay between hierarchy and contact splitting in biological adhesion highlighted through a hierarchical shear lag model, ArXiv 1710:09265. (2017).